

Metal Fragments and Extended Arrays on a Si(100)-(2×1) Surface. I. Theoretical Study of ML_n Complexation to Si(100)

Robert Konecny and Roald Hoffmann*

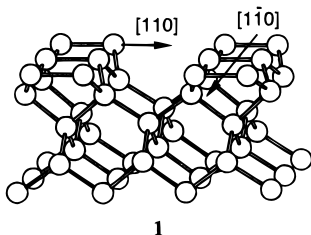
Contribution from the Department of Chemistry, Baker Laboratory, Cornell University, Ithaca, New York 14853-1301

Received April 15, 1999. Revised Manuscript Received June 28, 1999

Abstract: Adsorption of two model fragments, $Fe(CO)_4$ and $PdCl_3^-$, on a cluster model of the Si(100) surface and disilene was studied by means of density functional calculations. The reconstructed silicon–silicon surface dimer forms a strong bond to metal fragments, analogous to ethylene π -bond complexation to a transition metal complex. This bond can be described in terms of the Dewar–Chatt–Duncanson model. The $Fe(CO)_4$ fragment binds to the surface cluster model in two geometrical configurations—in a geometry in which the Si–Si bond is in the equatorial plane of an approximate trigonal bipyramid at Fe and another, less stable geometry with the Si–Si bond perpendicular to the equatorial plane. $PdCl_3^-$ also binds well, forming a square planar complex with the Si–Si bond in the plane of the complex. Since the Cl^- ligands in $PdCl_3^-$ are labile, adsorption in a geometry with the Si–Si bond perpendicular to the plane of the square planar complex leads to two unusual structures in which Si–Cl bonds are formed. The possibility of formation of one-dimensional chains of transition metal fragments on the surface, using O^{2-} and H^- bridging ligands has been explored.

Introduction

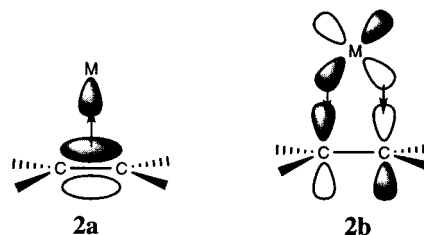
We have learned much about structure and reactivity of the simplest silicon surface, Si(100). The (2×1) reconstruction of this surface leads to formation of surface dimers, where two neighboring surface silicon atoms are connected by a σ bond (**1**). This still leaves a reactive, singly occupied orbital—a dangling bond—on each surface silicon atom. Two dangling bonds within one dimer interact, albeit weakly, and add a π component to the σ bond. The resultant weak double bond between two surface silicon atoms in the dimer plays an important role in controlling the properties and reactivity of the surface.



The double bond character of the Si(100) dimers relates them to molecular analogues, disilene (Si_2H_4) and the closely related and much more strongly π -bonded ethylene. There is a striking similarity between the reactivity of the Si(100) surface and that of disilene (or ethylene). Although the silicon–silicon double bond is weaker than the carbon–carbon double bond, both disilene and Si(100) surface undergo “classical” organic reactions, nucleophilic and electrophilic 1,2-additions, [2+2] cycloadditions, as well as Diels–Alder reactions.^{1–6}

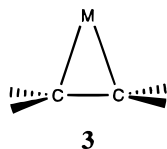
- (1) Weidenbruch, M. *Coord. Chem. Rev.* **1994**, *130*, 275–300.
 (2) Okazaki, R.; West, R. *Adv. Organomet. Chem.* **1996**, *39*, 231–273.
 (3) Waltenburg, H. N.; Yates, J. T., Jr. *Chem. Rev.* **1995**, *95*, 1589–1673.
 (4) Konecny, R.; Doren, D. J. *J. Am. Chem. Soc.* **1997**, *119*, 11098–11099.

One class of reaction which has not yet been explored experimentally or theoretically on the Si(100) surface is π -coordination of the surface double bond in an organometallic complex. η^2 -coordination of alkene double bonds is well-known in organometallic chemistry; the first organotransition metal compound, Zeise’s salt, $K^+ [PtCl_3(C_2H_4)]^-$ contains this kind of bond.⁷ The bond between a transition metal fragment and an ethylene is understood as a synergic donor–acceptor process: electrons are donated from the ethylene π orbital to a vacant metal orbital (**2a**), and at the same time electrons from an appropriate symmetry d_{π} metal orbital are back-donated to the empty π^* ethylene orbital (**2b**). This very useful bonding picture was first put forward by Dewar⁸ and by Chatt and Duncanson.⁹

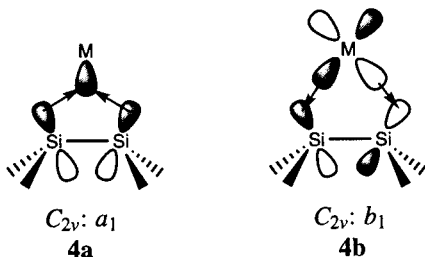


Another view of the interaction between a transition metal fragment and a ethylene is as a metallacycle (**3**). People have spent a lot of energy arguing about which of these bonding pictures is appropriate to one or another olefin complex; our own opinion is that it would be advisable to look at the bonding as a continuum of donation and acceptance, which encompasses both views.^{10–12}

- (5) Teplyakov, A. V.; Kong, M. J.; Bent, S. F. *J. Am. Chem. Soc.* **1997**, *119*, 11100–11101.
 (6) Konecny, R.; Doren, D. J. *Surf. Sci.* **1998**, *417*, 169–188.
 (7) Huheey, J. E.; Keiter, E. A.; Keiter, R. L. *Inorganic chemistry: principles of structure and reactivity*, 4th ed.; Harper Collins College Publishers: New York, NY, 1993.
 (8) Dewar, M. J. S. *Bull. Soc. Chim. Fr.* **1951**, *18*, C71–C79.
 (9) Chatt, J.; Duncanson, L. A. *J. Chem. Soc.* **1953**, 2939–2947.



Although olefin complex formation is common, analogous transition metal η^2 -disilene compounds were prepared only a few years ago.^{13–16} The η^2 -disilene complexes exhibit a rich chemistry, reacting with both nucleophilic and electrophilic reagents under relatively mild conditions.¹⁷ Theoretical studies of transition metal with η^2 -disilene bonded complexes have shown that the Dewar–Chatt–Duncanson picture is also quite applicable here, i.e., that both charge donation and back-donation contribute to the bond between the metal and disilene.^{18–20} Since the electronic structure of disilene is similar to that of the Si(100) surface dimer, a comparable bond should be formed between a transition metal fragment and the surface. The surface π -type orbital (HOMO) should be capable of donating electron density to an empty metal orbital (an a_1 interaction in C_{2v} symmetry, **4a**) and the surface π^* orbital (LUMO) could be involved in back-donation from the d_{π} metal orbital (a b_1 interaction in C_{2v} symmetry, **4b**).



There is another reason to be interested in the interaction of metal fragments with the silicon surface. A hypothetical reaction between the Si(100) surface and a number of transition metal fragments may lead to formation of a well-ordered monolayer of transition metal complexes on the surface. The adjacent metal atoms could also be connected through ligand bridges, in principle creating one-, two-, or three-dimensional ordered structures which might exhibit interesting physical properties. The ligands on the metal fragments might be labile, leading potentially to bare metal ordered arrays on the silicon.

In this paper we propose and study model interactions between a transition metal fragment and the Si(100) surface, as well as its molecular analogue, disilene. The formation of a one-dimensional chain of the transition metal fragments on the surface (by bridging neighboring metal adsorbates) is also investigated.

(10) Albright, T. A.; Hoffmann, R.; Thibault, J. C.; Thorn, D. L. *J. Am. Chem. Soc.* **1979**, *101*, 3801–3812.

(11) Pidun, U.; Frenking, G. *J. Organomet. Chem.* **1996**, *525*, 269–278.

(12) Frenking, G.; Pidun, U. *J. Chem. Soc., Dalton Trans.* **1997**, *10*, 1653–1662.

(13) Pham, E. K.; West, R. *J. Am. Chem. Soc.* **1989**, *111*, 7667–7668.

(14) Pham, E. K.; West, R. *Organometallics* **1990**, *9*, 1517–1523.

(15) Berry, D. H.; Chey, J. H.; Zipin, H. S.; Carroll, P. J. *J. Am. Chem. Soc.* **1990**, *112*, 452–453.

(16) Koloski, T. S.; Carroll, P. J.; Berry, D. H. *J. Am. Chem. Soc.* **1990**, *112*, 6405–6406.

(17) Sharma, H. K.; Pannell, K. H. *Chem. Rev.* **1995**, *95*, 1351–1374.

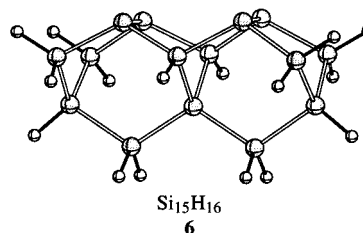
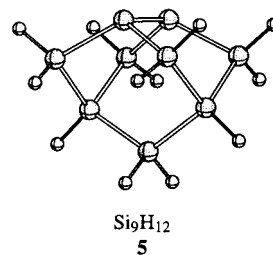
(18) Anderson, A. B.; Shiller, P.; Zarate, E. A.; Tessier-Youngs, C. A.; Youngs, W. J. *Organometallics* **1989**, *8*, 2320–2322.

(19) Sakaki, S.; Ieki, M. *Inorg. Chem.* **1991**, *30*, 4218–4224.

(20) Cundari, T. R.; Gordon, M. S. *J. Mol. Struct. (THEOCHEM)* **1994**, *313*, 47–54.

Theoretical Methods

General Procedure. The surface was approximated in density functional calculations by a cluster model consisting either of nine silicon atoms (single-dimer model, Si_9H_{12} , **5**) or 15 silicon atoms (double-dimer model, $Si_{15}H_{16}$, **6**). These cluster models provide an accurate representation of the geometry and energetics of the Si(100) surface.^{4,6,21,22}



The density functional calculations were carried out using the Amsterdam density functional (ADF) package version 2.3.^{23,24} The local density approximation (LDA) for exchange correlation used the parametrization of Vosko, Wilk, and Nusair (VWN)²⁵ and the Perdew–Wang’s nonlocal corrections (NLDA) for both exchange and correlation (PW91)²⁶ were added self-consistently. The numerical integration scheme adopted was the polyhedron method developed by te Velde et al.²⁷ with the accuracy parameter, ACCINT, of 4.0.

A set of uncontracted double- ζ Slater-type orbitals (STO) was employed for the main group atoms (H, C, O, Cl, Si), with single- ζ $3d$ (carbon, oxygen, chlorine, and silicon) or $2p$ (hydrogen) polarization for all ligand atoms. The Fe and Pd basis sets were triple- ζ with single- ζ polarization. The inner core shells were treated by the frozen core approximation, through Fe($3s$, $3p$), Pd($4s$, $4p$), C($1s$), O($1s$), Si($2p$), and Cl($2p$). A set of auxiliary s , p , d , f , and g STO functions, centered on all nuclei, was introduced to fit the molecular density and to represent Coulombic and exchange potentials accurately. The basis, core, and fit sets correspond to basis set III (H, C, O, Si, Cl) and basis set IV (Fe, Pd) of ADF 2.3, respectively.

All degrees of freedom of the studied systems were optimized. Convergence was deemed to be achieved when changes in coordinate values were less than 0.01 Å and the norm of all gradient vectors was smaller than 0.01. The NLDA DFT electron density analysis was performed using the Hirshfeld atomic charge partitioning schemes.^{28,29}

Bonding Energy Analysis. The bonding energy in the calculated complexes can be analyzed by the extended transition state method developed by Ziegler and Rauk.^{30–32} This approach is based on a decomposition of the bonding energy between two interacting fragments into different components. The total bonding energy (ΔE_b) can be

(21) Liu, Q.; Hoffmann, R. *J. Am. Chem. Soc.* **1995**, *117*, 4082–4092.

(22) Konecny, R.; Doren, D. J. *J. Chem. Phys.* **1997**, *106*, 2426–2435.

(23) Baerends, E. J.; Ellis, D. E.; Ros, P. *Chem. Phys.* **1973**, *2*, 41–51.

(24) Ravenek, W. In *Algorithms and Applications on Vector and Parallel Computers*; te Riele, H. J. J., Dekker, T. J., van de Vorst, H. A., Eds.; Elsevier: Amsterdam, 1987.

(25) Vosko, S.; Wilk, L.; Nusair, M. *Can. J. Phys.* **1980**, *58*, 1200–1211.

(26) Perdew, J. P.; Chevary, J.; Vosko, S.; Jackson, K. A.; Pederson, M. R.; Singh, D.; Fiolhais, C. *Phys. Rev. B* **1992**, *46*, 6671–6687.

(27) te Velde, G.; Baerends, E. J. *J. Comput. Phys.* **1992**, *99*, 84–98.

(28) Hirshfeld, F. *Theor. Chim. Acta* **1977**, *44*, 129–138.

(29) The Hirshfeld charge partitioning scheme divides the molecular charge density at each point among the several atoms in proportion to their free-atom densities at the corresponding distances from the nuclei.

Table 1. Structural Parameters (in Å and deg) and Bonding Energy for Fe(CO)₄ Binding to a Si₉H₁₂ Cluster and Disilene

	7a	7b	8a	8b
Fe–C	1.820 ^a , 1.819	1.814 ^a , 1.820	1.838 ^a , 1.811	1.812 ^a , 1.814
C–O	1.155 ^a , 1.153	1.157 ^a , 1.154	1.173 ^a , 1.157	1.160 ^a , 1.159
Si–Fe	2.496	2.455	2.435	2.345
Si–Si	2.326	2.280	2.342	2.353
Fe–C–O	178.2 ^a , 179.5	179.8 ^a , 179.2	164.0 ^a , 174.7	178.7 ^a , 176.0
Fe–Si–Si	62.2	62.3	61.3	127.5
Si–Fe–Si	55.5	55.3	57.5	
ΔE _b (kcal/mol)	–83.2	–88.9	–73.8	–53.1

^a Axial bond.

expressed as a sum of the steric energy ΔE_{ster} and the orbital interaction energy ΔE_{oi}:

$$\Delta E_b = \Delta E_{\text{ster}} + \Delta E_{\text{oi}} \quad (1)$$

The steric energy component in turn can be divided into two contributions, one being the electrostatic contribution (ΔE_{elstat}) due to the classical electrostatic interaction between the two unperturbed fragment charge distributions, the second the Pauli contribution (ΔE_{pauli}) due to the repulsive four-electron interaction between occupied orbitals:

$$\Delta E_{\text{ster}} = \Delta E_{\text{elstat}} + \Delta E_{\text{pauli}} \quad (2)$$

The orbital interaction energy arises from the interaction of occupied and empty orbitals on each fragment. This term can be partitioned by contributions from each symmetry representation Γ of the interacting fragments, and a small correction term accounting for numerical errors in the DFT calculation as implemented in the ADF code:

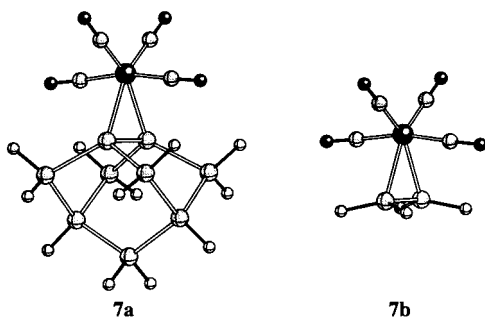
$$\Delta E_{\text{oi}} = \sum_{\Gamma} \Delta E_{\Gamma} + \Delta E_{\text{corr}} \quad (3)$$

To obtain the overall binding energy ΔE it is necessary to include the preparation energy, ΔE_{prep}. This is the energy required for deformation of fragments from their equilibrium structure to the conformation in the final complex:

$$\Delta E = \Delta E + \Delta E^{\text{prep}}$$

Interaction of Si(100) Models with Fe(CO)₄

To begin our study of the geometry and energetics of transition metal complex formation on the Si(100) surface a simple neutral bonding partner, Fe(CO)₄ was chosen. The fragment was positioned over two silicon atoms of the Si₉H₁₂ surface model with the axial CO ligands perpendicular to the silicon dimer bond, and a full geometry optimization was performed. The optimized geometry (**7a**) is shown below. A full geometry optimization was also performed on a simpler analogue of the surface complex, Fe(CO)₄(H₂Si=SiH₂), disilene modeling the surface dimer (**7b**). Important structural parameters of the optimized surface cluster and disilene complexes are presented in Table 1.



The geometries of both the disilene and surface model complexes are very similar, small differences arising only in

Table 2. Energy Decomposition for the Surface and Disilene Models (in kcal/mol)^a

	ΔE _{ster}	ΔE _{oi}			ΔE _b	
		ΔE _{a1}	ΔE _{a2}	ΔE _{b1}		
7a	30.9	–57.4	–2.4	–46.7	–7.6	–83.2
7b	31.3	–65.5	–2.0	–46.0	–7.4	–88.9
9a	38.5	–45.6	–3.4	–36.8	–10.8	–58.2
9b	37.5	–49.5	–2.1	–35.0	–9.2	–58.5

^a ΔE_{ster} is steric contribution, ΔE_{oi} is orbital interaction energy (with the contributions partitioned by symmetry type) and ΔE_b is total bonding energy.

the Si–Si and Si–Fe distances. The surface Si–Si bond length in the surface cluster model is 2.326 Å, a value that falls in the middle of the range expected for a double (2.242 Å calculated in a bare cluster silicon dimer) and a single bond (2.403 Å computed in the dihydrogenated silicon dimer). The double bond character of the surface Si–Si bond is clearly reduced upon coordination to the Fe(CO)₄ fragment in **7a**. A similar, although stronger, reduction in the double bond character is calculated for the disilene model. The Si–Si bond length in the disilene–Fe(CO)₄ model (2.280 Å) is closer to the computed single bond length in disilane (2.377 Å) than to the double bond length in disilene (2.127 Å). This calculated disilene Si–Si distance is similar to the experimentally observed 2.260 Å Si–Si distance in a closely related molecule, Cp₂W(Si₂Me₄).¹⁵

The bonding energy for the surface model complex **7a** is –83 kcal/mol, the bonding energy for the simpler disilene **7b** is slightly higher, –89 kcal/mol. This bonding energy, ΔE_b, is calculated as an interaction energy between two fragments (each calculated in the geometry they have in the final relaxed complex), the Fe(CO)₄ fragment in the singlet electronic configuration and either the Si₉H₁₂ or disilene fragment. The orbital interaction energy between fragments (ΔE_{oi}) can be partitioned by symmetry type. Since the optimized structures have C_{2v} symmetry (although no symmetry constraints were employed during the optimization), this symmetry was used to simplify the bonding energy analysis. The two most significant bonding contributions in the Fe(CO)₄/Si₉H₁₂ (**7a**) and Fe(CO)₄/disilene (**7b**) bonding energies are ΔE_{a1} and ΔE_{b1} (Table 2). The ΔE_{a1} contribution is bigger in the Fe(CO)₄/disilene model than in the Fe(CO)₄/Si₉H₁₂ model, which mainly accounts for the greater magnitude of total bonding energy in the disilene model.

The population of fragment orbitals with major contributions to the a₁ and b₁ interactions is shown in Table 3. We calculate a significant electron transfer in **7a** from the fully occupied surface π_{Si} orbital (9a₁) to the empty metal σ_M^{*} orbital (10a₁) and from the metal π_M orbital (6b₁) to the empty surface π_{Si}^{*} orbital (6b₁). These fragment orbitals are illustrated in Figure

(30) Ziegler, T.; Rauk, A. *Theor. Chim. Acta* **1977**, *46*, 1–10.(31) Ziegler, T.; Rauk, A. *Inorg. Chem.* **1979**, *18*, 1558–1565.(32) Ziegler, T.; Rauk, A. *Inorg. Chem.* **1979**, *18*, 1755–1759.

Table 3. Fragment Orbital Population for $Fe(CO)_4/Si_9H_{12}$ (**7a**), $Fe(CO)_4/Si_2H_4$ (**7b**), $PdCl_3^-/Si_9H_{12}$ (**9a**), and $PdCl_3^-/Si_2H_4$ (**9b**)^a

	a_1		b_1	
	metal fragment	Si fragment	metal fragment	Si fragment
7a	0.85($10a_1$)	1.81($8a_1$), 1.42($9a_1$)	1.38($6b_1$)	0.58($6b_1$)
7b	0.94($10a_1$)	1.95($1a_1$), 1.87($2a_1$), 1.20($3a_1$)	1.45($6b_1$)	0.51($2b_1$)
9a	1.88($5a_1$), 0.67($7a_1$)	1.90($8a_1$), 1.50($9a_1$)	1.95($1b_1$), 1.86($2b_1$), 1.69($3b_1$)	0.42($6b_1$)
9b	1.90($5a_1$), 0.75($7a_1$)	1.94($8a_1$), 1.34($9a_1$)	1.94($1b_1$), 1.89($2b_1$), 1.75($3b_1$)	0.37($6b_1$)

^a Only those fragment orbitals that change their orbital population by more than by 0.05 e^- as a result of coordination are shown.

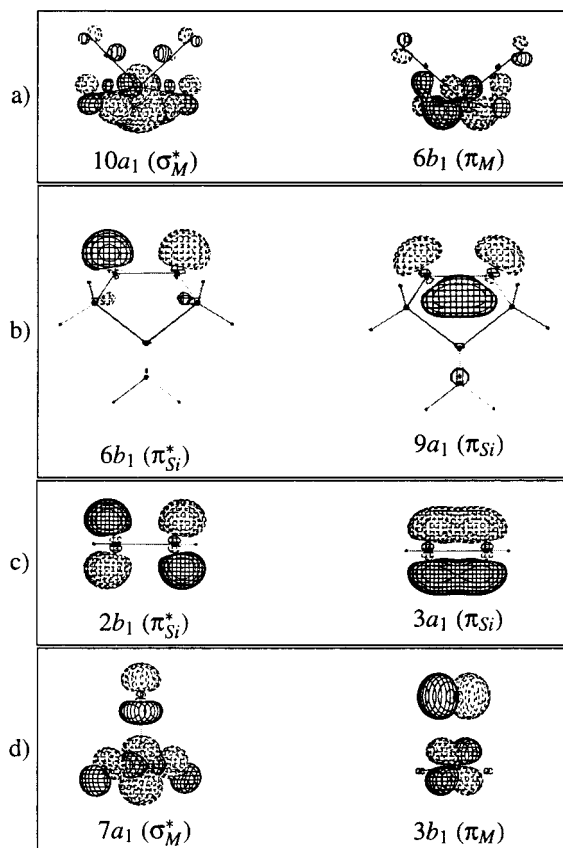


Figure 1. Important fragment orbitals of (a) $Fe(CO)_4$, (b) Si_9H_{12} , (c) disilene, and (d) $PdCl_3^-$ fragments. The orientation of the ML_n fragment corresponds to its geometry in **7** and **9**.

Table 4. Calculated Hirshfeld Charges on the Metal Fragment, Metal Center, and on Silicon Atoms in Disilene or on Surface Silicon Atoms in Si_9H_{12}

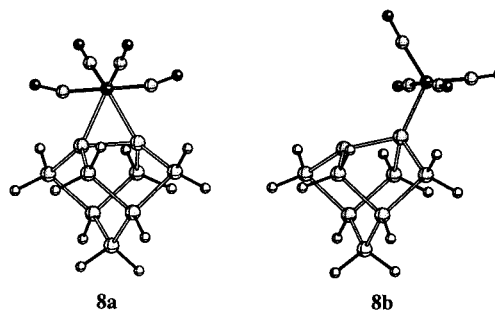
	7a	7b	9a	9b	12a	12b	13
Σ on metal fragment	-0.03	-0.12	-0.68	-0.88	-1.29	-1.19	-0.70
metal only	-0.11	-0.12	0.44	0.42	0.45	0.46	0.42
Si	0.02	0.18	-0.01	0.10	-0.01	-0.04	-0.02

1. The interactions indicated are the important components of the Dewar–Chatt–Duncanson model. A similar interaction is calculated for the $Fe(CO)_4$ /disilene complex (**7b**, Table 3), where the most significant charge transfer is from disilene π_{Si} orbital ($3a_1$) to the empty metal σ_M^* orbital ($10a_1$) and back-donation from the metal π_M orbital ($6b_1$) to the disilene π_{Si}^* orbital ($2b_1$). The important disilene orbitals are also shown in Figure 1c.

The calculated Hirshfeld charge distribution for the surface cluster and disilene $Fe(CO)_4$ complexes is shown in Table 4. There is a small calculated net electron transfer from the surface cluster model to the transition metal complex (0.03 e^-). The electron transfer is more pronounced in the disilene model (0.12 e^-). This suggests fairly well-balanced σ -donation and π -back-

donation in the surface cluster model and larger σ -donation than π -back-donation in the disilene model. In comparison, the Mulliken population analysis of $Fe(CO)_4/C_2H_4$ complex predicts net electron transfer in the opposite direction (from the metal fragment to ethylene), due to larger π -back-donation than σ -donation.³³

There is also another possible geometry for the adsorbate complex, one with the axial CO ligands parallel to or eclipsing the Si–Si dimer bond. The bonding energy for this conformation (**8a**) is -74 kcal/mol, 10 kcal/mol higher (less stable) than for the adsorbate geometry in the favored configuration with the axial CO groups perpendicular to the silicon dimer bond (**7a**). This reflects poorer π -bonding and larger steric interaction between the surface and the adsorbate in the eclipsed conformation.¹⁰ However, this energy loss is partially compensated by a bonding interaction between the carbon atoms of the axial CO ligands and the surface silicon model atoms. This Si–C distance is 2.242 Å, which is greater than the sum of the Si and C covalent radii (1.95 Å), but much shorter than a van der Waals contact. We think that the interaction between the surface and the axial CO carbon atoms shows up in deviation of the Fe–(C–O)_{axial} angle (164.0°) from linearity.



We have investigated another hypothetical adsorbate structure, a geometry with the metal atom bonded to one of the surface silicon atoms. The optimized structure in this geometry (**8b**) is 30 kcal/mol less stable than the calculated lowest energy structure **7a**, but it is a local minimum. The underlying surface dimer in the cluster model complex **8b** is buckled (tilted along the surface normal), as is observed^{34–37} and calculated^{22,38–41} for other surface dimer asymmetrically bonded complexes. The

(33) Eisenstein, O.; Hoffmann, R. *J. Am. Chem. Soc.* **1981**, *103*, 4308–4320.

(34) Bennet, S. L.; Greenwood, C. L.; Williams, E. M. *Surf. Sci.* **1993**, *290*, 267–276.

(35) Wang, Y.; Bronikowski, M. J.; Hamers, R. J. *Surf. Sci.* **1994**, *311*, 64–100.

(36) Shan, J.; Wang, Y.; Hamers, R. J. *J. Phys. Chem.* **1996**, *100*, 4961–4969.

(37) Hamers, R. J.; Wang, Y. *Chem. Rev.* **1996**, *96*, 1261–1290.

(38) Vittadini, A.; Selloni, A.; Casarin, M. *Phys. Rev. B* **1995**, *52*, 5885–5889.

(39) Konecny, R.; Doren, D. J. *J. Phys. Chem. B* **1997**, *101*, 10983–10985.

(40) Bacalzo, F. T.; Musaev, D. G.; Lin, M. C. *J. Phys. Chem. B* **1998**, *102*, 2221–2225.

(41) Brown, A. R.; Doren, D. J. *J. Chem. Phys.* **1999**, *110*, 2643–2651.

Table 5. Calculated Structural Parameters (in Å and deg) and Bonding Energy for Products of PdCl₃⁻ Adsorption on Si₉H₁₂ (**9a**) and Disilene (**9b**)

	9a	9b
Pd–Cl	2.404 ^a , 2.475	2.407 ^a , 2.500
Pd–Si	2.482	2.457
Si–Si	2.294	2.248
Si–Pd–Si	55.0	54.5
Pd–Si–Si	62.5	62.8
ΔE _b (kcal/mol)	-58.2	-58.5

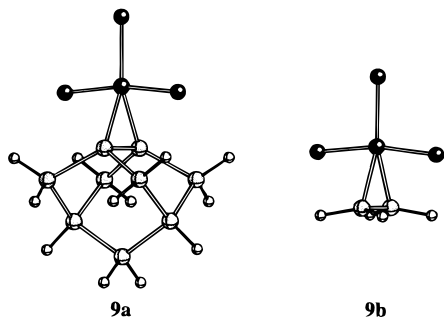
^a Axial position.

surface Si–Si bond is lengthened in both **8a** and **8b** compared to the Si–Si distance in **7a**, and the Fe–Si bond is shortened. There is a simple description of the bonding in **8a**, one consistent with the observed buckling. To attain an 18-electron configuration, the Fe(CO)₄ fragment desires an electron-pair Lewis base ligand (as in Fe(CO)₅ or Fe(CO)₄L). The surface model readily provides this by polarizing the weak R₂Si=SiR₂ double bond to R₂Si⁺–Si⁻R₂. The anionic Si end, which bonds as a base to Fe(CO)₄, is (as expected) more pyramidalized, the cationic end more planar.

These geometrical changes in the three structures, **7a**, **8a**, and **8b** represent three distinctive bonding modes of the Fe(CO)₄ fragment to the surface cluster model: strong and weak π coordination in **7a** and **8a**, respectively, and σ bonding in **8b**.

Interaction of Si(100) Models with PdCl₃⁻

The second prototypic transition metal fragment used in our study was PdCl₃⁻. We first optimized the geometry of a structure with the axial Cl ligands perpendicular to the Si–Si dimer bond (**9a**). The important geometrical parameters are presented in Table 5. The simpler analogue of the surface cluster adsorbate complex was also optimized (**9b**, Table 5). Again, there are only small geometrical differences between the disilene and surface cluster complex. The differences in the Pd–Si and Si–Si bond lengths are similar to the differences in the Fe(CO)₄/Si₉H₁₂ and Fe(CO)₄/disilene complexes. The Si–Si (2.248 Å) and Pd–Si (2.457 Å) distances in the disilene model are comparable to distances in a related, previously theoretically studied compound, PtCl₃⁻/disilene, with computed Si–Si 2.223 Å and Pt–Si 2.425 Å, respectively.^{19,20} The silicon–silicon bond in the surface cluster model (with the length of 2.294 Å) and in the disilene model (2.248 Å) is shorter than for corresponding Fe(CO)₄ model complexes.



The bonding energy between the palladium fragment and the silicon cluster model and disilene are very similar, -58 and -59 kcal/mol, respectively (Table 2). The dominating components of the bonding energy are again the ΔE_{a1} and ΔE_{b1} orbital interaction contributions. The lower bonding energy in PdCl₃⁻/Si₉H₁₂ compared to Fe(CO)₄/Si₉H₁₂ is due partly to the greater

Table 6. Calculated Overlaps for Important Fragment Orbitals

	7a Fe(CO) ₄ /Si ₉ H ₁₂	9a PdCl ₃ ⁻ /Si ₉ H ₁₂	7b Fe(CO) ₄ /Si ₂ H ₄	9b PdCl ₃ ⁻ /Si ₂ H ₄
a ₁ : ⟨10a ₁ 9a ₁ ⟩:	0.20	⟨10a ₁ 9a ₁ ⟩: 0.13	⟨10a ₁ 9a ₁ ⟩: 0.26	⟨10a ₁ 9a ₁ ⟩: 0.17
b ₁ : ⟨10a ₁ 9a ₁ ⟩:	0.29	⟨10a ₁ 9a ₁ ⟩: 0.11	⟨10a ₁ 9a ₁ ⟩: 0.35	⟨10a ₁ 9a ₁ ⟩: 0.12

Table 7. Calculated Structural Parameters (in Å and deg) and Bonding Energy for Products of PdCl₃⁻ Adsorption on the Si₉H₁₂ Cluster in the Eclipsed Conformation

	10	11
Si–Si	3.145	2.439
Si–Pd	2.325	2.307
Si–Cl	2.179	2.126
Pd–Cl	2.432	2.387
Si–Si–Pd	47.4	119.1
Si–Pd–Si	85.2	
Pd–Si–Cl	102.5	
Cl–Pd–Cl		172.2
Si–Pd–Cl	137.4	79.1, 108.7
ΔE _b (kcal/mol)	-113.1	-94.5

repulsive steric interaction and partly to a lower attractive orbital interaction. The latter effect is a consequence of the more contracted valence d orbitals in the positively charged Pd ion than in the Fe atom; this leads to a poorer overlap between d orbitals of the Pd ion and p orbitals of the surface model (Table 6). A similar trend (in the decrease of the bonding energy between a metal fragment and a π-ligand) is observed for Fe(CO)₄/C₂H₄ and PdCl₃⁻/C₂H₄ complexes. The C₂H₄ ligand is more strongly bound in Fe(CO)₄/C₂H₄ (experimental bonding energy 23 ± 3 kcal/mol)⁴² than in PdCl₃⁻/C₂H₄ (theoretically calculated bonding energy 12 kcal/mol).⁴³

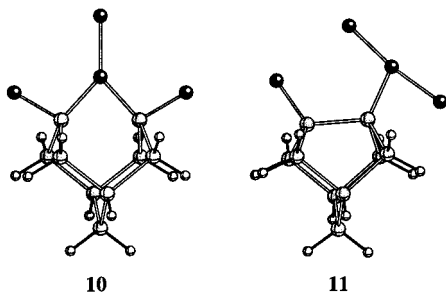
The population of the fragment orbitals most significantly involved in the a₁ and b₁ interactions is presented in Table 3. The biggest electron transfer in PdCl₃⁻/Si₉H₁₂ is calculated for the π_{Si} (9a₁) → σ_M^{*} (7a₁) donation and π_M (3b₁) → π_{Si}^{*} (6b₁) back-donation. These orbitals are depicted in Figure 1b and d. The most significant electron transfer in PdCl₃⁻/disilene is calculated for the π_{Si} (3a₁) → σ_M^{*} (7a₁) donation and π_M (3b₁) → π_{Si}^{*} (2b₁) back-donation. These interactions support again the Dewar–Chatt–Duncanson bonding picture.

The calculated Hirshfeld charge distribution for the disilene and surface cluster PdCl₃⁻ complexes is shown in Table 4. There is an overall electron transfer from the Pd fragment to the surface cluster model (0.32 e⁻). The electron transfer in the disilene model is predicted to be in the same direction (as that of the disilene fragment) but smaller (0.12 e⁻). The quite significant electron transfer from the metal fragment to both the Si₉H₁₂ and Si₂H₄ fragments indicates stronger contribution from π-back-donation than σ-donation. This is in contrast to well-balanced calculated contributions in the PdCl₃⁻/C₂H₄ complex.^{33,43}

We have also optimized a surface cluster–adsorbate complex starting in the “eclipsing” conformation, with the axial Cl ligands parallel to the Si–Si dimer bond. Surprisingly, we have found two quite different geometrical minima, depending on the starting geometry. In one the Si–Si bond and two Pd–Cl bonds are broken and two Si–Pd and two Si–Cl bonds are formed, **10** (Table 7). Si–Cl surface bonding is experimentally known, as in the studies of the reaction of Cl₂ with Si(100).^{3,44} In another

(42) Brown, D. L. S.; Connor, J. A.; Leung, M. L.; Paz-Andrade, M. I.; Skinner, H. A. *J. Organomet. Chem.* **1976**, *110*, 79–89.(43) Hay, P. J. *J. Am. Chem. Soc.* **1981**, *103*, 1390–1393.(44) Gao, Q.; Cheng, C. C.; Chen, P. J.; Choyke, W. J.; Yates, J. T. *J. Chem. Phys.* **1993**, *98*, 8308–8323.

isomer the surface silicon bond is retained during the optimization, but one of the Pd–Cl bonds is broken, and a Si–Cl bond is formed (**11**). Both of these structures are energetically lower than the adsorption product with the axial Cl ligands perpendicular to the surface Si=Si bond (**9a**). The geometry with the surface silicon bond broken (**10**) is more stable by 55 kcal/mol and the structure with the surface bond retained (**11**) by 36 kcal/mol than **9a**. Similar pathways are followed in the disilene complex.



These addition reactions leading to **10** and **11** do not change the formal oxidation state of the palladium ion, and they leave a 14 e^- configuration on the metal. These isomers should be susceptible to nucleophilic reactions, such as associative ligand substitution or oxidative addition at the unsaturated metal center.

Let us see if we make sense of what is going on in this system in organometallic terms. Structures of type **9a** are clearly analogous to Zeise's salt. There is no direct analogue to structures of type **10** (or reactions leading to them) in Zeise's salt chemistry, but some things may be said about the process. The reaction from **9a** to **11** (after rotation around a Pd–disilene bond) is the Si, Cl analogue of a β -hydride transfer.⁴⁵ The latter reaction is very well-known, although to our knowledge not yet exemplified for Si and Cl. **9a** going to **10** would be an extremely unusual reaction in carbon chemistry. It corresponds to a double migration of chlorides to a disilene that is split. Or it can be viewed as a double α -migration of chlorides from the metal. The strength of the carbon–carbon double bond precludes this reaction from being realized in organometallic carbon chemistry.

Another perspective on these systems is obtained by looking at the local geometry at the Pd. Fourteen electron d^8 systems (e.g., tricoordinate Au(III)) are classical Jahn–Teller situations.^{46,47} The trigonal (D_{3h}) ML_3 geometry is unstable relative to deformations to T- and Y-shaped structures.⁴⁸ In this context **11** clearly has a T-shaped geometry and **10** has a Y-shaped geometry, although the Pd local geometry in **10** is no doubt strongly influenced by geometry constraints imposed by the Si_9H_{12} cluster. To our knowledge there is no direct structural evidence for a Y-shaped Pd(II) compound.

Structure **11** with the Cl–Pd–Cl angle of 172° is more stable than a hypothetical structure with an angle of 90° by 20 kcal/mol. This is in agreement with a study by Tatsumi et al.⁴⁷ which predicts that a geometry PdA_2D^- with two more electronegative A substituents bonded to the metal opposite each other (A–Pd–A angle 180°) is more stable than a structure with an A–Pd–A angle of 90° .

(45) Collman, J. P.; Hegedus, L. S.; Norton, J. R.; Finke, R. G. *Principles and Applications of Organotransition Metal Chemistry*, 2nd ed.; University Science Books: Mill Valley, CA, 1987.

(46) Komiya, S.; Albright, T. A.; Hoffmann, R.; Kochi, J. K. *J. Am. Chem. Soc.* **1976**, *98*, 7255–7265.

(47) Tatsumi, K.; Hoffmann, R.; Yamamoto, A.; Stille, J. K. *Bull. Chem. Soc. Jpn.* **1981**, *54*, 1857–1867.

(48) Alvarez, S. *Coord. Chem. Rev.* **1999**, in press.

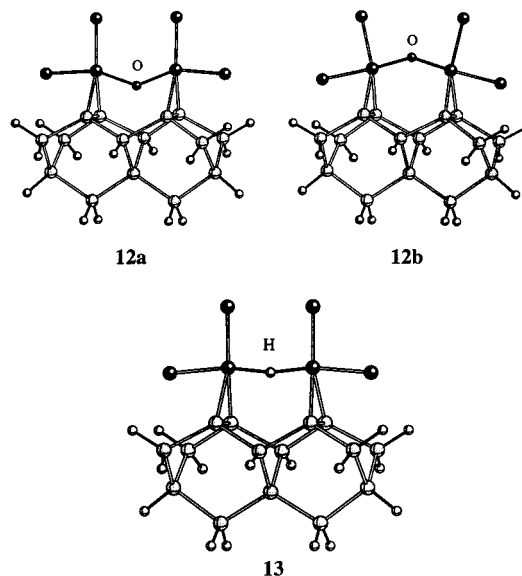
Table 8. Structural Parameters (in Å and deg) and Bonding Energy for $Pd_2Cl_4O^{2-}$ and $Pd_2Cl_4H^-$ Fragment Adsorption on the $Si_{15}H_{16}$ Cluster

	12a	12b	13
Pd–Cl	2.468 ^a , 2.486	2.522 ^a , 2.535	2.428 ^a , 2.431
Pd–Si	2.453	2.463	2.510
Si(1)–Si(1) ^b	2.300	2.300	2.279
Pd–Pd	3.975	3.849	3.766
Si(1)–Si(2) ^c	3.956	3.973	3.916
Pd–(O, H)	2.113	2.008	1.762
Pd–(O, H)–Pd	140.3	146.8	167.6
ΔE_b (kcal/mol)	–127.9	–132.8	–106.0

^a Axial position. ^b Intra-dimer Si–Si distance. ^c Inter-dimer Si–Si distance.

Toward the Formation of 1-D Transition Metal Fragment Chains on the Surface

To investigate the possible linkage of adjacent transition metal fragment adsorbates through a bridging ligand, a minimal model of a double-dimer cluster was used ($Si_{15}H_{16}$, **6**). Two $PdCl_2$ fragments were placed on the top of the double-dimer cluster in a geometry they would have in $PdCl_3^-/Si_9H_{12}$. The two palladium atoms were connected using either an O^{2-} ligand or smaller H^- ligand as the bridge. A full optimization was performed yielding structures **12a**, **12b** (O-bridged), and **13** (H-bridged). The important geometric parameters are presented in Table 8. Note that we have retained in these structures a Pd(II) and the rough Zeise's salt geometry at each Pd.



There are two minima for the structure with the O^{2-} bridge, one with the oxygen atom pointing down toward the surface cluster model (**12a**) and the other with the oxygen atom pointing up (**12b**). The bonding energy between the $Pd_2Cl_4O^{2-}$ fragment and the silicon double-dimer cluster is –128 and –133 kcal/mol for the **12a** and **12b** geometries, respectively. The binding in **12b** is thus –66 kcal/mol per one silicon dimer, which is somewhat stronger than the binding between $PdCl_3^-$ and a single silicon dimer cluster (**9a**). The bonding energy between the $Pd_2Cl_4H^-$ fragment and the double-dimer model in **13** is smaller, –106 kcal/mol. Although the geometry of the Pd–H–Pd bridge deviates slightly from linearity (168°), the energy needed to make the hydride bridge linear (Pd–H–Pd 180°) is only less than 1 kcal/mol.

There are only small geometrical differences between the structure with one PdCl_3^- fragment adsorbed on a single-dimer cluster and the structure with two PdCl_2 fragments connected through either O^{2-} or H^- bridges on the double-dimer cluster. The only significant change is in the Pd–Cl bond length elongation for both axial and equatorial Cl ligands. The biggest change (0.118 Å) is in the Pd–axial Cl length in **12b**.

The Pd–O bond lengths in **12a** (2.11 Å) and **12b** (2.01 Å) are comparable to the experimental Pd–O distance in similar bonding arrangement in $(\mu\text{-OH})_2$ bridged $(\text{Pd(II)})_2$ compounds (2.07–2.11 Å).^{49,50} The Pd–Pd separation in these complexes is shorter (2.98–3.14 Å) than in **12a** and **12b** (3.98 and 3.85 Å), accompanying a smaller Pd–O–Pd angle (90–99°) compared to the calculated Pd–O–Pd angle in **12a** and **12b** (140 and 147°).

The palladium–hydride distance in **13** (1.76 Å) is in the range of experimentally observed Pd–H bond lengths in $(\mu\text{-H})_2\text{Pd}_2$ compounds (1.62–1.79 Å).^{51,52} The known compounds are much more bent at H (Pd–H–Pd angle 109°).

Although the Pd–O–Pd angle in **12a** and **12b** is significantly different from 180°, this distortion from linearity is probably not caused by constraints imposed by the silicon double-dimer cluster geometry but rather by a geometrical preference of the O^{2-} bridging ligand itself. In fact, the Si double-dimer cluster geometry is quite flexible. The inter-dimer Si(1)–Si(2) distance is 4.003 Å in a bare double-dimer model, and is shortened upon bridge formation to 3.956 and 3.973 Å in **12a** and **12b**, respectively. The Pd–Pd distances in both **12a** and **12b** are comparable, shorter than the longest calculated Si(1)–Si(2) distance (4.003 Å). This suggests that the double-dimer model could accommodate a more linear Pd–O–Pd structure. In the hydride-bridged system (**13**) the Pd–Pd distance (3.766 Å) is shorter than the shortest calculated Si(1)–Si(2) distance (3.863 Å); since the H^- bridge is nearly linear there is probably some strain in the adsorbate structure. This strain may be responsible for the smaller bonding energy for **13** than in **12a** and **12b** (Table 8). It is important to note that the Si(1)–Si(2) distance in the real, more rigid Si(100) surface is 3.85 Å. This would cause more strain and consequently a smaller bonding energy than predicted in both the **12a** and **12b** structures.

(49) López, G.; Ruiz, J.; García, G.; Vicente, C.; Casabó, J.; Molins, E.; Miravilles, C. *Inorg. Chem.* **1991**, *30*, 2605–2610.

(50) Grushin, V. V.; Alper, H. *Organometallics* **1993**, *12*, 1890–1901.

(51) Fryzuk, M. D.; Lloyd, B. R.; Clentsmith, G. K. B.; Rettig, S. J. *J. Am. Chem. Soc.* **1991**, *113*, 4332–4334.

(52) Fryzuk, M. D.; Lloyd, B. R.; Clentsmith, G. K. B.; Rettig, S. J. *J. Am. Chem. Soc.* **1994**, *116*, 3804–3812.

Calculated Hirshfeld charges for **12a**, **12b**, and **13** are presented in Table 4. An electron transfer to the surface cluster model in the range from 0.30 to 0.36 and 0.41 e^- per one silicon dimer for **13**, **12a**, and **12b**, respectively, is calculated. This is comparable to the calculated electron transfer for the PdCl_3^- /single-dimer cluster model (0.32 e^-).

Conclusions

This theoretical study addresses for the first time bonding between a transition metal fragment and the Si(100) surface through coordination of the surface double bond to the metal.

Two model fragments, $\text{Fe}(\text{CO})_4$ and PdCl_3^- , bind effectively to our surface cluster models. The resulting bonding can be described in terms of the Dewar–Chatt–Duncanson model, where both charge donation from the HOMO of the surface to an empty metal orbital and back-donation from the d_π metal orbital to the empty π^* surface orbital play a key role. Other, less stable products are formed by adsorption of the $\text{Fe}(\text{CO})_4$ fragment on the Si_9H_{12} cluster model in the eclipsed conformation. The PdCl_3^- fragment contains more labile Cl^- ligands. Thus adsorption of PdCl_3^- has other channels available to it, effectively addition mechanisms. Two products result, one with the surface Si–Si bond retained and with a T-shaped Pd coordination, and the other with the Si–Si bond broken and a Y-shaped coordination of the palladium ion.

The bonding of disilene with the transition metal fragments is very similar to that of the Si(100) surface cluster model, leading to the formation of structurally and energetically comparable products. The similarity between the disilene and surface cluster model double bond reactivity suggests that principles of silicon and carbon organometallic chemistry could be applied to Si(100) surface chemistry, and vice versa.

Two transition metal fragments adsorbed on adjacent silicon dimers can be connected through a bridging ligand. Such bonding between two transition metal adsorbates, and bridged by an O^{2-} or H^- ligand, results in formation of stable products with some flexibility in the M–X–M adsorbate geometry. There are implications of this binding for the constructions of hypothetical one-, two-, or three-dimensional patterns on the surface, the properties of which are subject of our next study.

Since C(100) and Ge(100) surfaces also contain surface dimers with partial double-bond character, analogous reaction between organometallic fragments and these surfaces should be also feasible.

Acknowledgment. We are grateful to the National Science Foundation for its support of our research through grant CHE 94-08455.

JA991200H